

DNA passes through cohesin's hinge as well as its Smc3-kleisin interface

James E Collier and Kim A Nasmyth*

Department of Biochemistry, University of Oxford, Oxford, United Kingdom

Summary

The ring model (Haering et al. 2002) proposes that sister chromatid cohesion is mediated by co-entrapment of sister DNAs inside a tripartite cohesin ring created by a pair of rod-shaped proteins (Smc1 and Smc3) whose two ends are connected through dimerization of their hinges at one end and by association of their ATPase domains at the other end with the N- and C-terminal domains of a kleisin subunit (Scc1). The model explains how Scc1 cleavage triggers anaphase (Uhlmann, Lottspeich, and Nasmyth 1999) but has hitherto only been rigorously tested using small circular mini-chromosomes in yeast, where crosslinking the ring's three interfaces, creating a covalent circular molecule, induces catenation of individual sister DNAs (Haering et al. 2008; Srinivasan et al. 2018). If the model applies to real chromatids, then the ring must have a DNA entry gate essential for mitosis. Whether this is situated at the Smc3/Scc1 (Murayama and Uhlmann 2015; Murayama et al. 2018) or Smc1/Smc3 hinge (Gruber et al. 2006) interface is an open question. Using an in vitro system (Collier et al. 2020), we show that cohesin in fact possesses two DNA gates, one at the Smc3/Scc1 interface and a second at the Smc1/3 hinge. Unlike the Smc3/Scc1 interface, passage of DNAs through SMC hinges depends on both Scc2 and Scc3, a pair of regulatory subunits necessary for entrapment in vivo (Srinivasan et al. 2018). This property together with the lethality caused by locking this interface but not that between Smc3 and Scc1 in vivo (Gruber et al. 2006) suggests that passage of DNAs through the hinge is essential for building sister chromatid cohesion. Passage of DNAs through the Smc3/Scc1 interface is necessary for cohesin's separase-independent release from chromosomes (Chan et al. 2012) and may therefore largely serve as an exit gate.

Introduction

The sister chromatid cohesion essential for mitosis and meiosis is mediated by a pair of rod-shaped SMC proteins (Smc1 and Smc3) joined together through an interaction between hinge domains at one end. The interconnection by a kleisin subunit (Scc1) of their ATPase domains at the other end creates a ring-like structure within which it is proposed sister DNAs are entrapped during DNA replication (Haering et al. 2002). Two approaches have hitherto been used to test the ring model. The first has been

a method to induce thiol-specific chemical crosslinks within the three interfaces of SMC-Kleisin (S-K) rings. An early version of this approach showed that covalent circularization by BMOE of a version of cohesin containing cysteine pairs within the ring's interfaces is sufficient to cause catenation of small circular sister DNAs that are otherwise not inter-twined, hence proving their co-entrapment (Haering et al. 2008). Furthermore, analysis of a wide variety of strains carrying different cohesin mutations has subsequently confirmed that catenation in this manner of sister minichromosome DNAs correlates with the ability of yeast cells to proliferate (Srinivasan et al. 2018).

The second approach has been to elucidate the mechanism by which DNAs enter S-K rings. The logic being that only when we have understood this mechanism and found it to operate inside cells could we be certain that entrapment does indeed form the basis of cohesion. The initial goal was to establish which of the cohesin rings' three interfaces must open up to let in DNA, in other words to identify cohesin's DNA entry gate. The finding that inter-connection of Smc1 and Smc3 hinges using rapamycin (when FKBP12 and FRB were inserted into small loops within the Smc1/3 hinges) blocked cohesion establishment while fusion of Smc3 or Smc1 with Scc1 did not do so led to the proposal that if cohesin has a unique essential DNA entry gate, then it must be at the hinge interface (Gruber et al. 2006). However, these experiments merely showed that a modification predicted to hinder hinge opening blocks establishment of cohesion, which is not the same as proving that DNAs actually enter via this interface. Besides which, the conclusion that the hinge is a DNA entry gate is not universally accepted (Murayama and Uhlmann 2015; Murayama et al. 2018). Thus, despite being crucial for understanding how cohesion is established, the location of cohesin's DNA entry gate remains unresolved. To break this impasse, we recently developed an in vitro assay to measure entrapment of DNAs within S-K rings, using the same technique used in vivo, namely catenation of circular DNAs by cysteine-substituted cohesin rings chemically circularized using BMOE (Collier et al. 2020). S-K DNA entrapment in vitro is stimulated by Scc2 and depends on ATP and Scc3 but not on Pds5 or Wapl, reflecting the properties of S-K entrapment in vivo (Srinivasan et al. 2018), suggesting the reaction is physiologically relevant. Using this system, we now describe experiments that show definitively that cohesin possesses two gates through which DNAs pass, at least in vitro, one at the Smc3/Scc1 interface and a second at the Smc1/3 hinge. We also describe a series of topological assays suggesting that the first step is passage of DNAs between cohesin's ATPase heads and their enclosure by Scc2 in the lower half of an SMC compartment bounded by hinges and heads engaged by ATP.

68 **Covalent closure of cohesin ring interfaces**

69 Cohesin's DNA gate(s) could in principle be identified merely by observing the process of entrapment
70 in real time. Because this is not at present technically possible, we instead covalently sealed each ring
71 interface shut in a manner orthogonal to the thiol-specific crosslinking protocol that we use to measure
72 entrapment (Collier et al. 2020). This approach allows us to seal potential DNA gates prior to the
73 entrapment process. If DNA entered through a single gate, then sealing should block entrapment.
74 Though such a result would be consistent with the gate being used for entrapment, it would not directly
75 demonstrate passage, as the sealing process could in principle also interfere with passage through a
76 different gate, by somehow altering the latter's conformation. Crucially, a failure to block entrapment
77 by sealing a single ring interface would imply that the interface in question is either not a gate or that
78 that it is not the sole entry gate. Through a striking result, blocking entry would therefore permit only
79 weak conclusions. A more rigorous approach would be to seal two out of the ring's three interfaces,
80 leaving only a single potential gate. In this case, continued entrapment would demonstrate that DNA
81 must have passed through the sole remaining interface.

82
83 To seal the Smc3/Sccl interface, we expressed a fusion protein in which the N-terminus of Sccl is
84 connected by a short linker to the C-terminus of Smc3 (S3 fusion; Figure 1A, Figure 1 - supplement
85 1A). A similar approach was used connect Sccl's C-terminus to Smc1's N-terminus, thereby sealing the
86 Smc1/Sccl interface (S1 fusion). Smc1 and Smc3 hinges cannot be connected using this approach
87 because they are located within the middle of their polypeptides. In this case, we achieved highly
88 efficient covalent closure using an isopeptide bond created between a spytag and a spycatcher domain
89 (Li et al. 2014) inserted into loops on the surface of Smc1 and Smc3 hinges respectively (Hinge fusion;
90 Figure 1A, Figure 1 - supplement 1A & B). We next created three types of cohesin complexes
91 composed of a single polypeptide in which two out of three interfaces were covalently sealed, namely a
92 Smc3-Sccl-Smc1 (S3 S1 fusion) fusion containing a wild type hinge interface, a Smc3-Sccl fusion
93 whose hinge was connected to that of Smc1 using a spytag-spycatcher pair (S3 Hinge fusion), and a
94 Sccl-Smc1 fusion whose hinge was similarly connected to that of Smc3 (S1 Hinge fusion). Lastly, we
95 created a covalently circular ring in which all three interfaces were sealed (Circular cohesin).
96 Remarkably, all seven types of cohesin rings produced abundant and stable complexes (Figure 1B &
97 C). Some had modestly reduced rates of ATP hydrolysis, with circular cohesin having the greatest
98 defect (~ 60 % that of WT cohesin; Figure 1 - supplement 1C).

99
100 **DNA passes through the Smc1/Smc3 hinge as well as the Smc3/Sccl interface**

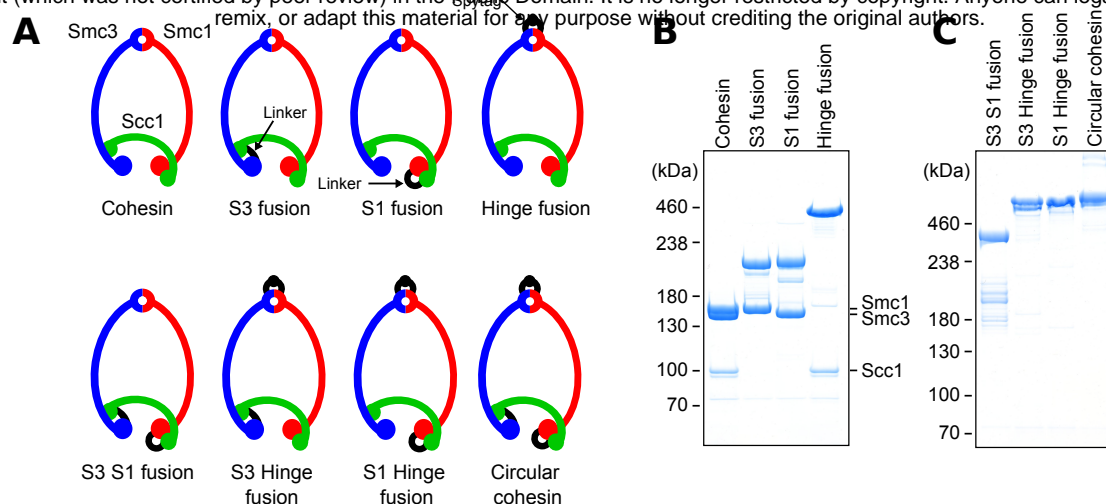


Figure 1. Covalent closure of cohesin's interfaces. (A) SMC-kleisin rings, showing their three interfaces. Those connected by a covalent linkage are marked in black. (B) Coomassie stain of purified cohesin with either the Smc3/Scc1 (S3 fusion), Scc1/Smc1 (S1 fusion), or hinge interfaces (Hinge fusion) covalently sealed. (C) Coomassie stain of purified cohesin with two or three interfaces covalently sealed.

Fig 1

Linker Sequences <https://doi.org/10.1101/2022.05.30.494034>; this version posted May 30, 2022. The copyright holder has placed this preprint (which was not certified by peer review) in the public domain. It is made available under aCC-BY 4.0 International license.

Smc3 Spycatcher insertion

ARGSGSGGSSVTTLSGLSGEQGPSGDMTTEEDSATHIKFSKRDEGRELATMEL
RDSSGKTISTWISDGHVKDFYLYPGKYTFVETAAPDGYEVATPIEFTVNEDGQVTVDG
EATEGDAHTSSGSGSGSAS

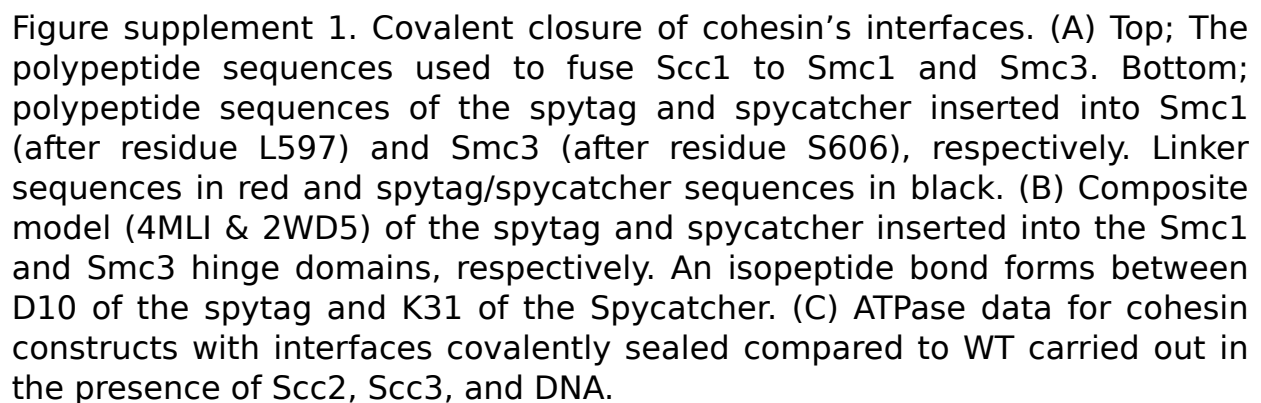


Fig S1

101 We next tested the ability of these different fusion proteins to entrap circular plasmid DNA in vitro
 102 (Figure 2 – supplement 2A; Collier et al. 2020). As expected from in vivo results (Gruber et al. 2006;
 103 Srinivasan et al. 2018), DNAs were entrapped by the cohesin rings containing either the Smc3-Scc1 or
 104 Scc1-Smc1 fusions. More surprising, they were also entrapped by rings with the Hinge fusion (Figure
 105 2A). It is difficult to make direct comparisons between the efficiencies as entrapment by each version
 106 depends on different cysteine pair combinations, whose crosslinking by BMOE can vary. We can
 107 nevertheless conclude that DNA enters the cohesin ring via at least two different gates. To identify
 108 these, we measured entrapment by rings with two interfaces sealed, whereby DNA can only enter
 109 through the one remaining open interface. These assays revealed ATP-dependent DNA entrapment by
 110 cohesin rings containing the Smc3-Scc1-Smc1 fusion (S3 S1 fusion) as well as rings containing the
 111 Scc1-Smc1-Hinge fusions (S1 Hinge fusion; Figure 2B). However, DNA was not entrapped by a
 112 complex with the Smc3-Scc1-Hinge fusions (S3 Hinge fusion). These observations demonstrate that
 113 DNA entrapment arises by passage through the hinge as well as through the Smc3/Scc1 interfaces.
 114 Importantly, no passage occurs through the Smc1/Scc1 interface, at least when the other two gates are
 115 covalently sealed.

116

117 Scc2 is required for DNA passage through the hinge but not through the Sm3/Scc1 interface

118 Entrapment within S-K rings in vivo normally depends on both Scc2 and Scc3. We therefore addressed
 119 whether hinge or Smc3/Scc1 gate passage in vitro shares this property. Entrapment by the Smc3-Scc1-
 120 Smc1 fusion was abolished by omission of either regulatory protein (Figure 2C). Entrapment via the
 121 hinge in vitro therefore resembles in vivo entrapment. This suggests that the reason why cohesion
 122 establishment is abolished by linkage of Smc1 and Smc3 hinges containing FRB and FKBP12
 123 respectively using rapamycin (Gruber et al. 2006) is because passage of DNA through the hinge is an
 124 essential step. Interestingly, the strict dependence of hinge-mediated entrapment on Scc2 differs from
 125 entrapment by wild type S-K rings in vitro, which still occurs in the absence of Scc2, albeit at a
 126 reduced level (Figure 2 – supplement 2B; Collier et al. 2020). A simple explanation for this difference
 127 is that cohesin entraps DNA via both hinge and Smc3/Scc1 pathways in vitro and the Scc2-independent
 128 entrapment is due entirely to passage through the Smc3/Scc1 gate. If so, sealing the Smc3/Scc1 gate
 129 should abolish Scc2-independent S-K entrapment. As predicted, entrapment by rings containing the
 130 Smc3-Scc1 fusion depends on Scc2 as well as Scc3 (Figure 2D). In other words, Scc2-independent
 131 entrapment requires a Smc3/Scc1 gate that can be opened.

132

133 To address whether entrapment via the Smc3/Scc1 gate is affected by Scc2, we measured the effect of
 134 Scc2 and Scc3 on entrapment of DNA by cohesin whose hinge alone is fused and contains cysteine

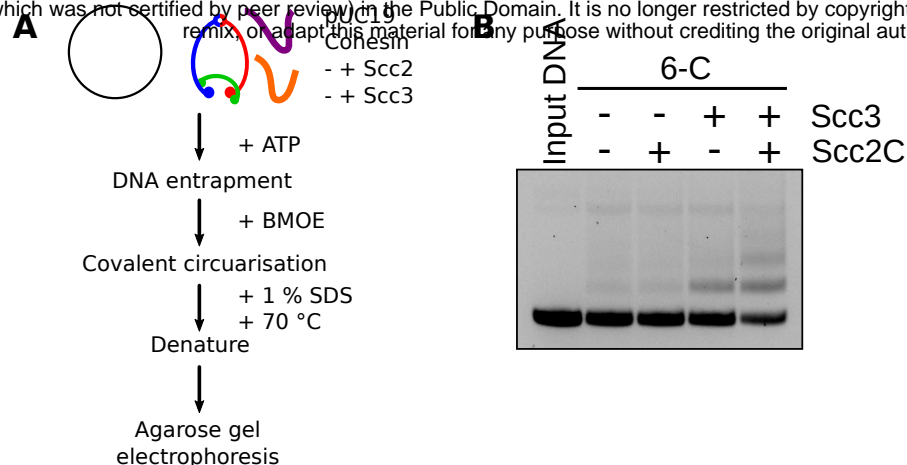


Figure supplement 2. DNA passes through cohesin's hinge and Smc3/Scc1 interfaces. (A) Schematic of the in vitro entrapment assay. (B) DNA entrapment for WT cohesin (6C) in the presence or absence of Scc2 and Scc3.

Fig S2

135 pairs within both SMC-Scc1 interfaces. Because DNA cannot pass through the Smc1/Scc1 interface, all
 136 entrapment by such cohesin must be via its Smc3/Scc1 interface. Entrapment by this construct depends
 137 on Scc3 but not Scc2 (Figure 2E). The dependence of DNA passage through the Smc3/Scc1 interface
 138 on Scc3 but not Scc2 in vitro resembles the activity that dissociates cohesin from chromosomes in vivo,
 139 a process dependent on Wapl and also blocked by the Smc3-Scc1 fusion (Chan et al. 2012). It is
 140 therefore possible that our in vitro experiments capture this process, albeit acting in reverse, as
 141 previously suggested (Murayama and Uhlmann 2015). In vivo, release not only does not require Scc2
 142 but is actively blocked by it, at least in G1 cells (Srinivasan et al. 2019). Given that passage of DNA
 143 through the Smc3/Scc1 interface is not required for cell proliferation, for S-K entrapment in vivo, or
 144 even for cohesin's stable association with the bulk of the genome, it is uncertain whether passage of
 145 DNA through this gate has any role in building cohesion in addition to its well documented role in
 146 mediating release.

147

148 **DNAs entrapped in SMC compartments in the absence of Scc3 are located between Scc2 and** 149 **engaged heads**

150 Given that passage of DNA through the hinge may be essential for building cohesion, the strict
 151 dependence of this process on Scc2 raises a question as to Scc2's role. Reactions performed in the
 152 absence of Scc3 provide an important clue. Under these circumstances, Scc2 promotes rapid
 153 entrapment of DNA within cohesin's SMC compartment (Figure 3 – supplement 3A), namely between
 154 the hinge and Smc1 and Smc3 head domains engaged in the presence of ATP (Collier et al. 2020).
 155 Crucially, this process is not accompanied by entrapment within S-K rings (Collier et al. 2020). Cryo-
 156 EM structures of DNA oligonucleotides bound to Scc2 and cohesin suggest that DNA trapped within
 157 SMC compartments by Scc2 binds simultaneously to Scc2 and a groove created by the engagement of
 158 Smc1 and Smc3 heads in the presence of ATP (PDB 6ZZ6). DNA associates with similar grooves
 159 above the engaged heads of condensin (Lee, Rhodes, and Lowe 2022), MukBEF (Burmann et al. 2021),
 160 and Rad50 (Kashammer et al. 2019), implying that this type of association is a highly conserved feature
 161 of SMC-like ATPase domains. In the case of cohesin, the DNA is actually “clamped” in a small
 162 compartment created by association of Scc2's N-terminal and central domains bound to Smc3's neck
 163 and head domains respectively (Collier et al. 2020; Higashi et al. 2020; Shi et al. 2020). Though the
 164 conditions under which these cryo-EM structures were obtained resemble those necessary for
 165 entrapment of DNA within the SMC compartment, namely both require Scc2, ATP, and DNA, but not
 166 Scc3 or ATP hydrolysis (Collier et al. 2020), we cannot be certain whether the two activities are truly
 167 synonymous. What is required is a crosslinking assay for DNA clamping comparable to the one used to
 168 measure SMC compartment entrapment.

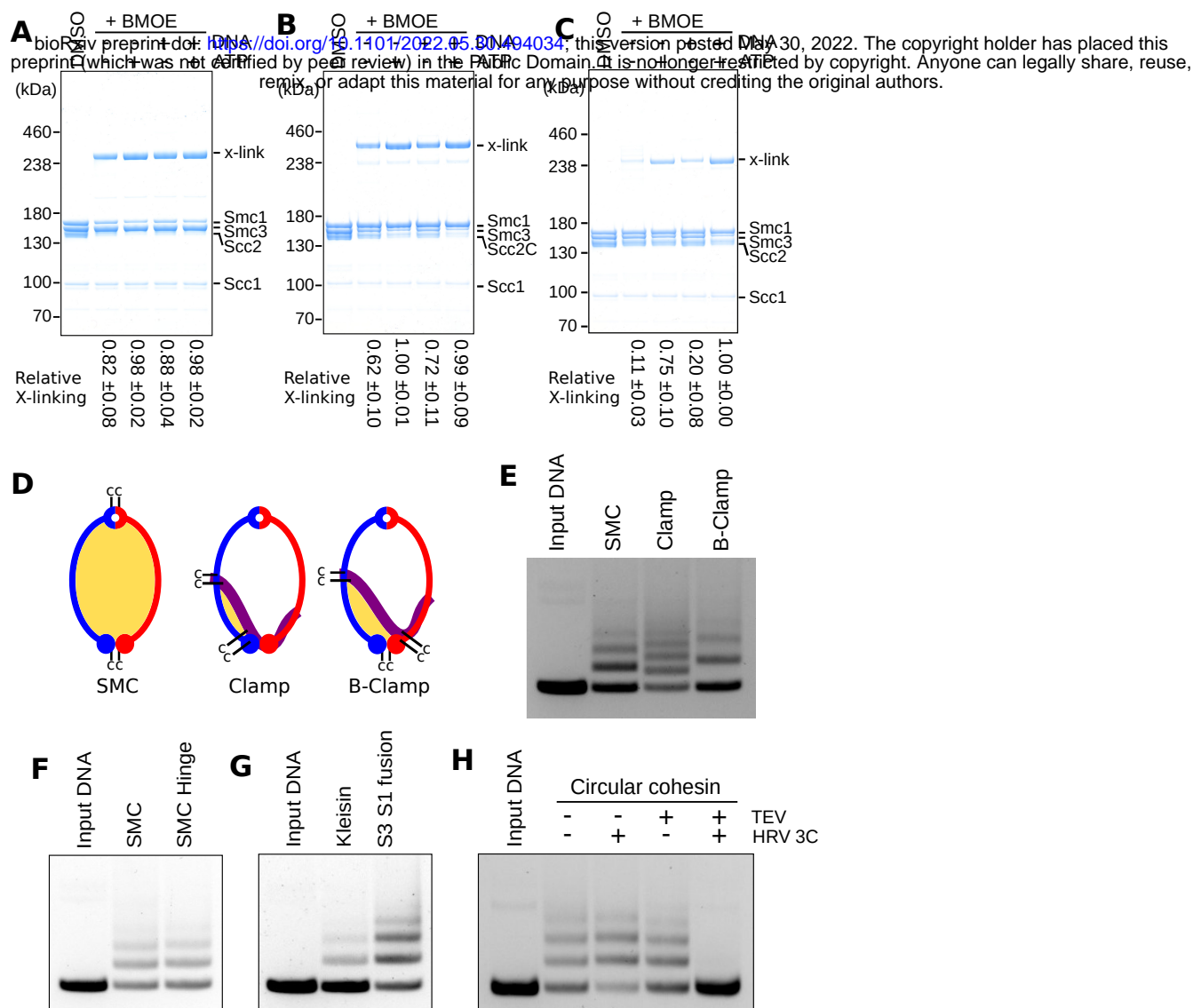


Figure 3. DNA passes through cohesin's ATPase domains. (A) Crosslinking of Scc2 to the Smc1 head in the presence or absence of ATP and DNA. (B) Crosslinking Scc2 to the Smc3 head in the presence or absence of ATP and DNA. (C) Crosslinking Scc2 to the Smc3 neck in the presence or absence of ATP and DNA. (D) Models of cohesin showing either the SMC, Clamp, or below the clamp (B-Clamp) compartments, highlighted in yellow. For Clamp and B-Clamp compartments Scc2 is in purple. (E) Entrapment of DNA in either the SMC, Clamp, or below the clamp (B-Clamp) compartments, in the presence of Scc2 after a 2 min incubation. (F) Entrapment of DNA in the SMC compartment by cohesin with either a WT hinge (SMC) or with the hinge covalently fused (SMC Hinge) in the presence of Scc2 after a 2 min incubation. (G) Entrapment of DNA in the kleisin compartment by cohesin with either both kleisin interfaces open (Kleisin) or covalently closed (S3 S1 fusion) in the presence of Scc2 after a 2 min incubation. (H) Entrapment of DNA by covalently circular cohesin in the presence of Scc2 after a 2 min incubation. After crosslinking, BMOE was quenched by addition of DTT and then the samples were treated with TEV and/or HRV 3C proteases and incubated at 24 °C for 30 min.

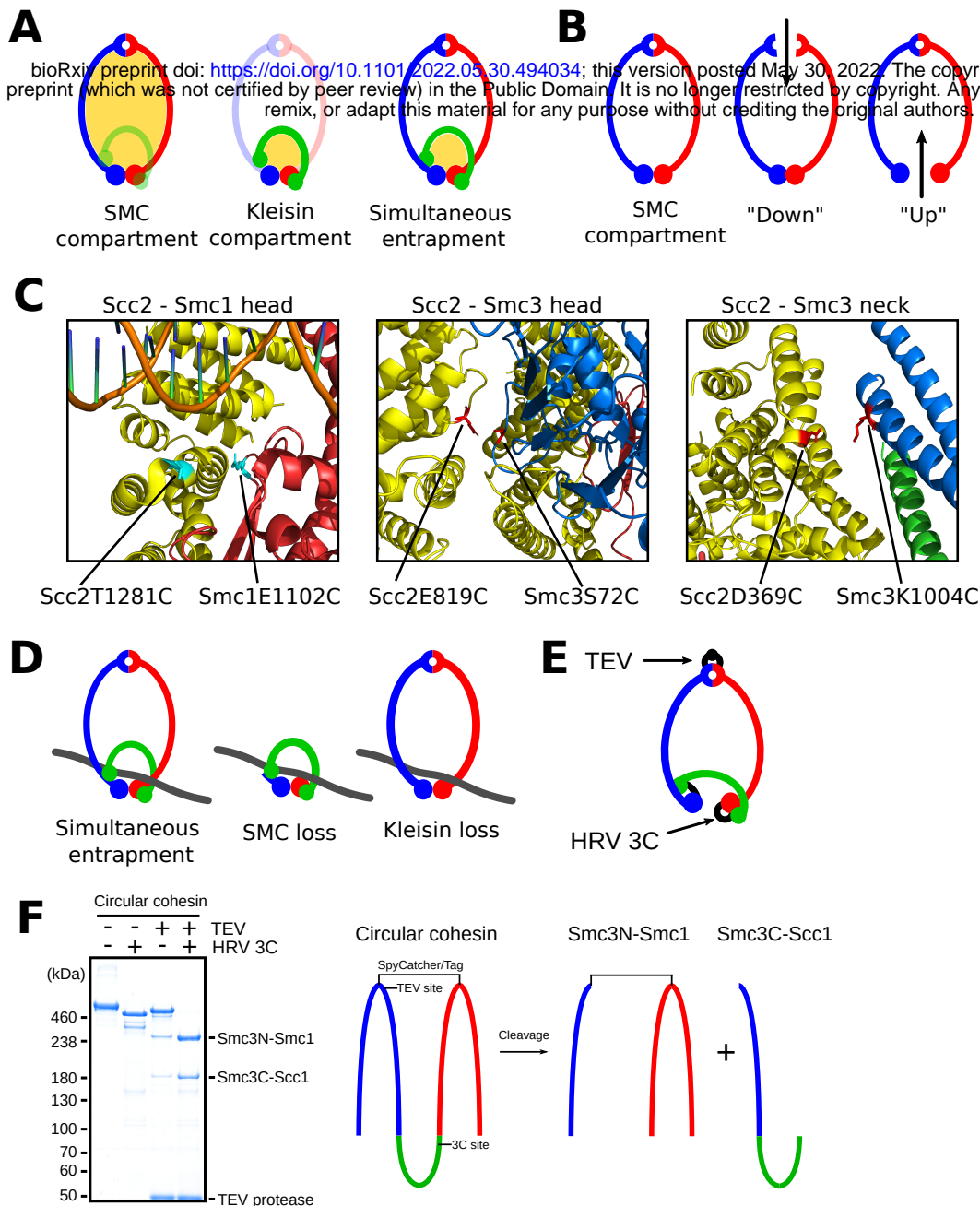


Figure supplement 3. DNA passes through cohesin's ATPase domains. (A) Models showing the SMC compartment, Kleisin compartment and the overlap between SMC and kleisin compartments, as highlighted in yellow. (B) DNA could enter the SMC compartment by going "down" through the hinge, or "up" through the heads. (C) Left panel showing the cysteine crosslinking pair to crosslink Scc2 to the Smc1 head. Middle panel showing the cysteine crosslinking pair to crosslink Scc2 to the Smc3 head. Right panel showing the cysteine crosslinking pair to crosslink Scc2 to the Smc3 neck. (D) Entrapment through the heads would lead to entrapment in both the SMC and kleisin compartments. If DNA were lost from the SMC compartment, it would still be entrapped in the kleisin compartment, and vice versa. (E) A TEV protease site is located in the linker between the spycatcher and the C-terminal half of Smc3. A HRV 3C protease site is located in the linker between Scc1 and Smc1. (F) Left panel; Coomassie stain of covalently circular cohesin incubated with either TEV and/or HRV 3C proteases for 1 hour at 30 °C in the combinations indicated. Right panel; Schematic showing the polypeptide topology of covalently circular cohesin and the position of the protease cleavage sites. Incubation with both TEV and HRV 3C proteases will cleave the construct into a ~180 kDa C-terminal-Smc3-Scc1 fragment and an N-terminal-Smc3-Smc1 fragment.

169

170 We therefore designed a set of cysteine pairs within Scc2-SMC interfaces that could be crosslinked by
171 BMOE if DNA were clamped in the manner observed in the cryo-EM structure (Figure 3 – supplement
172 3C). To this end, cysteines were introduced into the interfaces between Scc2 and the Smc1 head
173 (Scc2T1281C Smc1E1102C), between Scc2 and the Smc3 head (Scc2E819C Smc3S72C), and between
174 Scc2 and Smc3’s neck (Scc2D369C Smc3K1004C). As predicted by the cryo-EM structure, all three
175 pairs enabled BMOE to crosslink Scc2 to SMC heads in the presence of ATP and DNA (Figure 3A - C).
176 Crosslinking between Scc2 and either Smc1 or Smc3 head occurred in the absence of both ATP and
177 DNA but was stimulated by ATP, an effect that was more pronounced for crosslinking between Scc2
178 and the Smc3 head. DNA also modestly increased crosslinking between both cysteine pairs, but only in
179 the absence of ATP. In contrast, crosslinking between Scc2 and the Smc3 neck was strongly ATP
180 dependent and enhanced by DNA (Figure 3C). These results suggest that Scc2 initially binds to the
181 Smc1 head, subsequently binds the Smc3 head, and only binds the Smc3 neck efficiently upon the
182 engagement of Smc1 and Smc3 heads in the presence of ATP and DNA.

183

184 We next created two different cysteine pair combinations to measure clamping using our DNA
185 entrapment assay. The first combined Scc2D369C Smc3K1004C with Scc2E819C Smc3S72C, whose
186 simultaneous crosslinking should entrap DNA in a covalent compartment formed by crosslinks between
187 the N-terminal and central domains of Scc2 with Smc3’s neck and head respectively (the clamp;
188 Figure 3D). The second combined Scc2D369C Smc3K1004 and Scc2T1281C Smc1E1102C with
189 Smc1N1192C Smc3R1222C, a pair specific for engaged heads. Simultaneous crosslinking of all three
190 interfaces should entrap DNA in a compartment created by Scc2’s association with both Smc1 and
191 Smc3 heads when they are engaged (Below the clamp or B-clamp; Figure 3D). Under the same
192 conditions that promote entrapment in the SMC compartment, namely the presence of Scc2 and ATP,
193 and the absence of Scc3, DNA was efficiently entrapped in both clamp and B-clamp compartments
194 within 2 min (Figure 3D & E).

195

196 **Entrapping DNA in the SMC and kleisin compartments involves passing DNA between ATPase** 197 **head domains**

198 DNA could enter the SMC compartment by passage “down” through an opened hinge or “up” between
199 SMC heads (Figure 3 – supplement 3B). To distinguish these, we analysed the effect of pre-sealing the
200 hinge interface. This had no effect on SMC entrapment, excluding the possibility that DNA passes
201 “down” through the hinge (Figure 3F). If DNA instead passes between the ATPase heads, without any
202 dissociation of Scc1 from either the Smc3 neck or Smc1 head, then entrapment within the SMC

203 compartment will be accompanied by entrapment between engaged heads and the kleisin subunit
 204 associated with them; i.e. in the kleisin compartment, which we have previously shown (Collier et al.
 205 2020). However, it could be argued that entrapment in the kleisin compartment does not arise in this
 206 manner but rather as a result of a separate transport process in which DNA passes between a transiently
 207 opened SMC/kleisin interface either before or during head engagement. Indeed, such a mechanism has
 208 been invoked to explain clamping of DNA on top of engaged heads by Mis4, the *S. pombe* Scc2
 209 ortholog (Higashi et al. 2020). To address whether kleisin disengagement is required for entrapment
 210 between engaged heads and their associated kleisin, we introduced the cysteine pair specific for
 211 engaged heads (Smc1N1192C Smc3R1222C) into the Smc3-Scc1-Smc1 fusion. Sealing both kleisin
 212 interfaces did not prevent entrapment within the kleisin compartment. In fact, this construct entrapped
 213 DNA even more efficiently than WT (Figure 3G), presumably because only one single interface needs
 214 to be crosslinked compared to the three required for WT. Clearly, entrapment within the kleisin
 215 compartment in the presence of Scc2 does not involve passage through either Smc1/ or Smc3/kleisin
 216 gates. We conclude that the only interface that must open for entrapment of DNA within the SMC or
 217 kleisin compartments is that between the Smc1 and Smc3 ATPase heads.

218
 219 Due to the identical conditions upon which entrapment in the SMC and kleisin compartments takes
 220 place (Collier et al. 2020), it is likely that entrapment in these two compartments is a consequence of a
 221 single reaction and that passage of DNA through the head domains leads to simultaneous entrapment of
 222 DNA in both the SMC and kleisin compartments (Figure 3 – supplement 3A & D). If true, cohesin with
 223 all three interfaces fused should still be able to entrap DNA in the SMC and kleisin compartments.
 224 Furthermore, cleavage of either the SMC or kleisin compartments should have no effect on the amount
 225 of DNA entrapped, as DNA will remain entrapped within the remaining intact compartment (Figure 3 –
 226 supplement 3D). Only simultaneous cleavage of both compartments should release DNA. To test this,
 227 we created a version of the covalently circular species of cohesin containing the cysteine pair necessary
 228 to crosslink the heads when engaged in the presence of ATP. A pair of tandem TEV protease cleavage
 229 sites were inserted in the linker connecting the spycatcher and the Smc3 hinge, which enables cleavage
 230 of the SMC compartment, while an HRV 3C protease site was present in the linker connecting Scc1 to
 231 Smc1, which enables cleavage of the kleisin compartment (Figure 3 – supplement 3E). Incubating this
 232 construct with either TEV or HRV 3C leads to the linearization and opening of the SMC and kleisin
 233 compartments, respectively, while incubation with both proteases leads to opening of both
 234 compartments, as well as release of a ~180 kDa digestion fragment comprised of the C-terminal half of
 235 Smc3 fused to Scc1 (Figure 3 – supplement 3F). Circular cohesin was able to entrap DNA following
 236 the BMOE treatment that crosslinks engaged heads (Figure 3H) and remarkably entrapment was largely

unaffected by incubation with either TEV or HRV 3C proteases after crosslinking. DNA was only released upon incubation with both proteases. These results imply that DNA is simultaneously entrapped in both the SMC and kleisin compartments due to a single transportation process that involves DNA passage between the Smc1 and Smc3 head domains prior to their engagement. Furthermore, these results allow us to infer the path of Scc1, which must pass over and “above” the DNA, as has been suggested for condensin’s Brn1 subunit (Lee, Rhodes, and Lowe 2022).

Discussion

In summary, we have shown that cohesin has two DNA gates, one at the hinge and a second at the Smc3/Scc1 interface. Available evidence suggests that the hinge gate is essential for the establishment of sister chromatid cohesion while the Smc3/Scc1 gate is not. Future studies will be required to evaluate whether passage of DNA through the Smc3/Scc1 gate has any *in vivo* role in addition to releasing cohesin from chromosomes. Passage of DNA through the hinge is likely preceded by and very possibly dependent on its entrapment in a clamp between Scc2 and engaged ATPase heads (Figure 4A), a state created by passage of DNA between the SMC ATPase heads but not through either the hinge or Smc3/Scc1 gate. Following clamping, a section of DNA downstream of the clamp might then be passed through the hinge in a process dependent on Scc3. Passage through the Smc3/Scc1 interface occurs in the absence of Scc2 and may be the result of DNA binding to Scc3 during ATP-driven kleisin disengagement (Figure 4B).

Hitherto, our assay has only detected individual DNAs entrapped inside S-K rings. Entrapment of this nature occurs prior to DNA replication *in vivo* and is possibly converted to co-entrapment of sister DNAs during S phase with the help of specific replisome proteins (Srinivasan et al. 2020). Crucially, conversion of cohesin that has associated with unreplicated DNA to a form that co-entraps sister DNAs does not require Scc2. If as our *in vitro* experiments suggest, Scc2 is essential for passage of DNAs through the hinge, then co-entrapment arising during conversion cannot involve any further passage of DNA through the hinge gate. It either involves the Smc3/Scc1 gate (neither Smc3/Scc1 opening nor conversion are essential) or arises from an activity that somehow pulls replicated DNAs through the ring without it being re-opened.

Our assay measuring entry through the hinge *in vitro* will enable the identification of mutants specifically defective in this process and these can subsequently be used to address whether passage of DNA through the hinge has roles in chromosome topology besides cohesion establishment, for example, in holding together TAD boundaries associated with convergent CTCF sites (Liu and Dekker

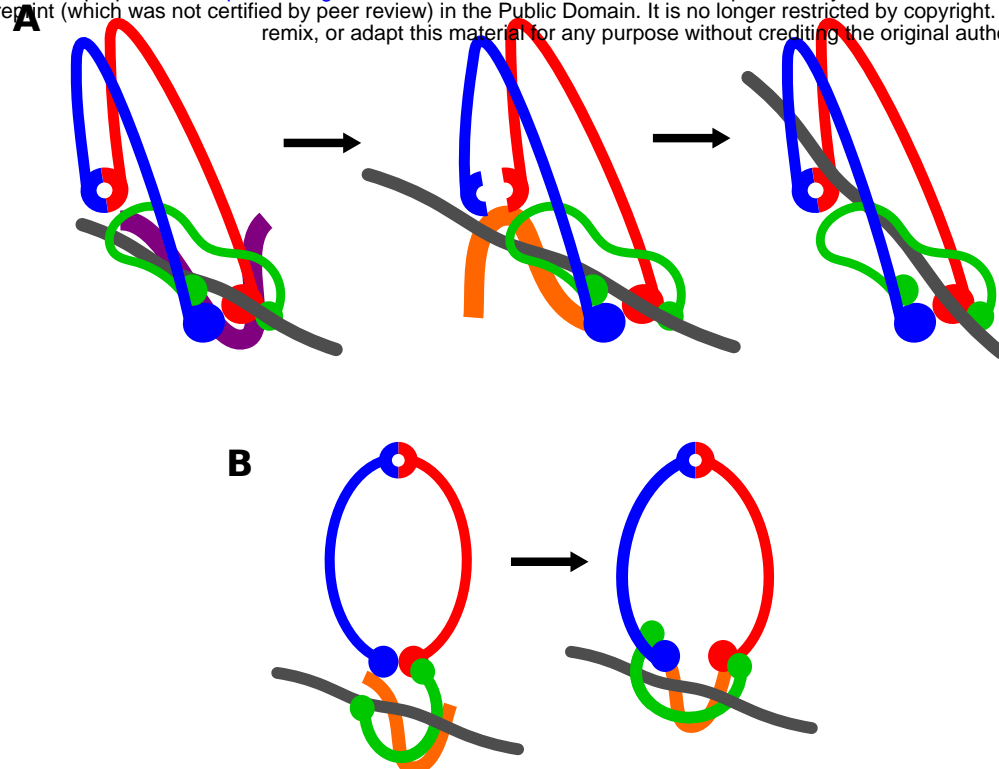


Figure 4. Models for DNA entry. (A) Model for DNA passage through the hinge. Scc2 (purple) first clamps DNA against the Smc3 neck. Scc3 (orange) is involved in opening and passing a downstream section of DNA through the hinge. (B) Model for DNA passage through the Smc3-Scc1 interface. ATP binding leads to the opening of the Smc3-Scc1 interface. DNA then binds to Scc3 and the interfaces closes.

2021). SMC hinge domains have two interfaces (north and south) and their dimerization creates a toroidal structure with a narrow lumen that is invariably positively charged (Kurze et al. 2011). Opening, either at one or both north and south interfaces (Gruber et al. 2006; Shi et al. 2020) would enable DNA to bind to highly conserved lysines residing inside the Smc1 hinge (Srinivasan et al. 2018), and this might be an important intermediate stage of the entrapment process. Whether the hinges of SMC complexes besides cohesin also act as DNA gates or whether their positively charged lumens merely bind DNA without passing it inside the ring is an important open question.

References

- Burmann, F., L. F. H. Funke, J. W. Chin, and J. Lowe. 2021. 'Cryo-EM structure of MukBEF reveals DNA loop entrapment at chromosomal unloading sites', *Mol Cell*, 81: 4891-906 e8.
- Chan, K. L., M. B. Roig, B. Hu, F. Beckouet, J. Metson, and K. Nasmyth. 2012. 'Cohesin's DNA Exit Gate Is Distinct from Its Entrance Gate and Is Regulated by Acetylation', *Cell*, 150: 961-74.
- Collier, J. E., B. G. Lee, M. B. Roig, S. Yatskevich, N. J. Petela, J. Metson, M. Voulgaris, A. Gonzalez Llamazares, J. Lowe, and K. A. Nasmyth. 2020. 'Transport of DNA within cohesin involves clamping on top of engaged heads by Scc2 and entrapment within the ring by Scc3', *Elife*, 9.
- Gruber, S., P. Arumugam, Y. Katou, D. Kuglitsch, W. Helmhart, K. Shirahige, and K. Nasmyth. 2006. 'Evidence that loading of cohesin onto chromosomes involves opening of its SMC hinge', *Cell*, 127: 523-37.
- Haering, C. H., J. Lowe, A. Hochwagen, and K. Nasmyth. 2002. 'Molecular Architecture of SMC Proteins and the Yeast Cohesin Complex', *Mol Cell*, 9: 773-88.
- Haering, C.H., A. Farcas, P. Arumugam, J. Metson, and K. Nasmyth. 2008. 'The cohesin ring concatenates sister DNAs.', *Nature*, 454 297-301.
- Higashi, T. L., P. Eickhoff, J. S. Sousa, J. Locke, A. Nans, H. R. Flynn, A. P. Snijders, G. Papageorgiou, N. O'Reilly, Z. A. Chen, F. J. O'Reilly, J. Rappsilber, A. Costa, and F. Uhlmann. 2020. 'A Structure-Based Mechanism for DNA Entry into the Cohesin Ring', *Mol Cell*, 79: 917-33 e9.
- Kashammer, L., J. H. Saathoff, K. Lammens, F. Gut, J. Bartho, A. Alt, B. Kessler, and K. P. Hopfner. 2019. 'Mechanism of DNA End Sensing and Processing by the Mre11-Rad50 Complex', *Mol Cell*, 76: 382-94 e6.
- Kurze, A., K. A. Michie, S. E. Dixon, A. Mishra, T. Itoh, S. Khalid, L. Strmecki, K. Shirahige, C. H. Haering, J. Lowe, and K. Nasmyth. 2011. 'A positively charged channel within the Smc1/Smc3 hinge required for sister chromatid cohesion', *EMBO J*, 30: 364-378.
- Lee, B. G., J. Rhodes, and J. Lowe. 2022. 'Clamping of DNA shuts the condensin neck gate', *Proc Natl Acad Sci U S A*, 119: e2120006119.

- Li, L., J. O. Fierer, T. A. Rapoport, and M. Howarth. 2014. 'Structural analysis and optimization of the covalent association between SpyCatcher and a peptide Tag', *J Mol Biol*, 426: 309-17.
- Liu, Y., and J. Dekker. 2021. 'Biochemically distinct cohesin complexes mediate positioned loops between CTCF sites and dynamic loops within chromatin domains', *bioRxiv*, 2021.08.24.457555.
- Murayama, Y., C. P. Samora, Y. Kurokawa, H. Iwasaki, and F. Uhlmann. 2018. 'Establishment of DNA-DNA Interactions by the Cohesin Ring', *Cell*, 172: 465-77 e15.
- Murayama, Y., and F. Uhlmann. 2015. 'DNA Entry into and Exit out of the Cohesin Ring by an Interlocking Gate Mechanism', *Cell*, 163: 1628-40.
- Shi, Z., H. Gao, X. C. Bai, and H. Yu. 2020. 'Cryo-EM structure of the human cohesin-NIPBL-DNA complex', *Science*, 368: 1454-59.
- Srinivasan, M., M. Fumasoni, N. J. Petela, A. Murray, and K. A. Nasmyth. 2020. 'Cohesion is established during DNA replication utilising chromosome associated cohesin rings as well as those loaded de novo onto nascent DNAs', *Elife*, 9.
- Srinivasan, M., N. J. Petela, J. C. Scheinost, J. Collier, M. Voulgaris, B. Roig M, F. Beckouet, B. Hu, and K. A. Nasmyth. 2019. 'Scc2 counteracts a Wapl-independent mechanism that releases cohesin from chromosomes during G1', *Elife*, 8.
- Srinivasan, M., J. C. Scheinost, N. J. Petela, T. G. Gligoris, M. Wissler, S. Ogushi, J. E. Collier, M. Voulgaris, A. Kurze, K. L. Chan, B. Hu, V. Costanzo, and K. A. Nasmyth. 2018. 'The Cohesin Ring Uses Its Hinge to Organize DNA Using Non-topological as well as Topological Mechanisms', *Cell*, 173: 1508-19 e18.
- Uhlmann, F., F. Lottspeich, and K. Nasmyth. 1999. 'Sister chromatid separation at anaphase onset is promoted by cleavage of the cohesin subunit Scc1p', *Nature*, 400: 37-42.

Materials and Methods

Reagents

ATP (Sigma)	Cat # 11140965001
BMOE (Thermo Scientific)	Cat # 22323
HRV 3C protease (Pierce)	Cat # 88946
TEV protease (Invitrogen)	Cat # 12575023
EnChek phosphate assay kit (Invitrogen)	Cat # E6646

Plasmids

pJC 93	pACEbac1 Smc1 Smc3 Scc1-StrepII
pJC 95	pACEbac1 Smc1 G22C K639C Smc3 E570C S1043C Scc1-StrepII A547C
pJC 153	pACEbac1 Smc1 K639C N1192C Smc3 E570C R1222C Scc1-StrepII
pJC 154	pACEbac1 Smc1 G22C N1192C Smc3 S1043C R1222C Scc1-StrepII A547C
pJC 127	pACEbac1 Smc1 G22C K639C Smc3Scc1-StrepII E570C A547C
pJC 123	pACEbac1 Smc3 E570C S1043C Scc1Smc1-StrepII K639C
pJC 106	pACEbac1 Smc1 G22C L597ST Smc3 S1043C S606SC Scc1-StrepII A547C
pJC 132	pACEbac1 Smc3Scc1Smc1-StrepII E570C K639C
pJC 129	pACEbac1 Smc1 G22C L597ST Smc3Scc1-StrepII S606SC A547C
pJC 124	pACEbac1 Smc3 S1043C S606SC Scc1Smc1-StrepII ST
pJC 135	pACEbac1 Smc3Scc1Smc1-StrepII S606SC TEV R1222C L597ST N1192C
pJC 151	pACEbac1i Smc1-His E1102C Smc3 Scc1-StrepII
pJC 100	pACEbac1i Smc1 Smc3 S72C Scc1-StrepII
pJC 101	pACEbac1i Smc3 K1004C Smc1 Scc1-StrepII
pJC 102	pACEbac1i Smc1 Smc3 S72C K1004C Scc1-StrepII
pJC 105	pACEbac1i Smc1 E1102C N1192C Smc3 K1004C R1222C Scc1-StrepII

pJC 69	pACEbac1 dN132-Scc2-StrepII
pJC 75	pACEbac1 dN132-Scc2-StrepII T1281C
pJC 77	pACEbac1 dN132-Scc2-StrepII E819C
pJC 76	pACEbac1 dN132 Scc2-StrepII D369C
pJC 78	pACEbac1 dN132-Scc2-StrepII D369C E819C
pJC 80	pACEbac1 dN132-Scc2-StrepII D369C T1281C
pJC 84	pACEbac1 StrepII-Scc3

376
377
378

379 **DNA and protein preparation.**

380 Protein and DNA components were prepared as described in Collier et al. 2020.

381

382 **ATPase assay**

383 DNA was prepared in DNA buffer (25 mM HEPES pH 7.5, 1 mM TCEP and 5% glycerol) by
384 annealing two complementary single-stranded 40 bp oligonucleotides by heating to 95 °C for 5 min and
385 decreasing in 0.1 °C intervals every 15 s to a final temperature of 4 °C. 150 µl reactions were prepared
386 containing 50 nM cohesin (Smc1, Smc3, Scc1), Scc3, Scc2, and 600 nM DNA in loading buffer (25
387 mM HEPES pH 7.5, 50 mM NaCl, 1 mM MgCl₂, 1 mM TCEP and 5% glycerol), and EnzChek
388 phosphate assay kit components (Invitrogen) added to their recommended concentrations. Reactions
389 were initiated by the addition of ATP (Sigma) to a concentration of 1 mM. The ATPase reaction was
390 followed by measuring the increase in absorbance at 360 nm over 60 min. Data shown an average of
391 three experiments.

392

393 **DNA entrapment assay**

394 13 µl reactions were prepared containing 165 nM cohesin and 9.3 nM supercoiled pUC19 in loading
395 buffer (25 mM HEPES pH 7.5, 50 mM NaCl, 1 mM MgCl₂, 1 mM TCEP and 5% glycerol). When
396 present, Scc3 was added to a concentration of 165 nM and Scc2 to a concentration of 55 nM. Reactions
397 were initiated by the addition ATP (Sigma) to a concentration of 5 mM. Reactions were incubated at 24
398 °C for either 40 min or 2 min at 750 rpm. Crosslinking was carried out by addition of 1.5 µl BMOE
399 (Thermo Scientific) to a concentration of 0.64 mM and incubated on ice for 6 min. Samples were then

denatured by addition of 1.5 μ l 10 % SDS and then incubated at 70 °C for 20 min at 750 rpm. DNA loading dye was then added and samples separated by agarose gel electrophoresis at 50 V for 17 hours at 4 °C. Assays were repeated at least twice.

When cleaving the SMC and kleisin compartments of circular cohesin 10 mM DTT was added after BMOE crosslinking and the samples incubated at 24 °C for 5 min. Protein cleavage was carried out by addition of 1 μ l TEV protease (Invitrogen) to cleave the SMC compartment and 1 μ l HRV 3C protease (Pierce) to cleave the kleisin compartment. To samples in which one or both proteases was omitted, loading buffer was added instead. Samples were then treated as in other experiments.

Protein crosslinking assay

10 μ l reactions were prepared containing 0.7 μ M cohesin (Smc1, Smc3 and Scc1) and Scc2 in loading buffer (25 mM HEPES pH 7.5, 50 mM NaCl, 1 mM $MgCl_2$, 1 mM TCEP and 5% glycerol). When present, ATP (Sigma) was added to a concentration of 10 mM and DNA (supercoiled pUC19) added to a concentration of 60 nM. Reactions were incubated at 24 °C for 5 min and then either 1 μ l DMSO added, or 1 μ l BMOE (Thermo Scientific) added to a concentration of 0.64 mM. Samples were then denatured by addition of 4x LDS protein loading dye and heated at 70 °C for 10 min. Samples were then separated by SDS-PAGE using 3-8 % tris-acetate gels ran at 100 V for 4 hr 30 min at 4 °C.

Circular cohesin cleavage

10 μ l samples were prepared containing 0.7 μ M circular cohesin. Protein cleavage was carried out by addition of 1 μ L TEV protease (Invitrogen) to cleave the SMC compartment and 1 μ L HRV 3C protease (Pierce) to cleave the kleisin compartment. To samples in which one or both proteases was omitted, loading buffer was added instead. Samples were then denatured by addition of 4x LDS protein loading dye and heated at 70 °C for 10 min. Samples were then separated by SDS-PAGE using 3-8 % tris-acetate gels ran at 100 V for 4 hr 30 min at 4 °C.